

Anomalous features of particle production in high-multiplicity events of pp collisions at the LHC energies

Samrangy Sadhu and Premomoy Ghosh*

Variable Energy Cyclotron Centre, HBNI, 1/AF Bidhan Nagar, Kolkata 700 064, India

(Dated: January 23, 2019)

Prevalent models of multi-particle production in relativistic pp collisions at pre-LHC energies, fail to provide convincing explanations to certain significant features of the final-state charged particles in high-multiplicity pp events at the LHC. This article presents a study, contrasting those features, usually interpreted as collective behaviour of particle production in relativistic heavy-ion collisions, in the framework of hydrodynamic EPOS3 model, emphasizing quantitative comparison between the data and the model-based simulation in the same kinematic ranges, for better cognizance of the data. The work reveals quantitative mismatch between the data and the model.

PACS numbers: 13.85.Hd, 25.75-q

I. INTRODUCTION

The experiments at the Relativistic Heavy Ion Collider (RHIC), through satisfactory description of the flow-like behaviour of particle production in relativistic heavy-ion collisions by relativistic hydrodynamics [1], established [2–5] formation of collective medium in such collisions. Suppression of high- p_T particles, revealed in terms of relative yield of charged particles in heavy-ion collisions compared to pp collisions at the same centre-of mass energy, identified the collective medium as thermalized medium of Quark-Gluon Plasma (QGP) [6, 7]. Reconfirming the formation of QGP with heavier ions at higher collisional energies, the experiments at the Large Hadron Collider (LHC), reported flow-like features of particle productions, in high-multiplicity events of pp collisions, in contrast to the present understanding of particle production in relativistic pp collisions, based on the data at the pre-LHC energy range. It is the so-called “ridge” structure in the long range near side angular correlations in high-multiplicity events of proton-proton collisions at $\sqrt{s} = 7$ TeV that first reported [8] the anomaly in particle productions in pp collisions at the LHC. Further experimental studies [9–11] at $\sqrt{s} = 7$ and 13 TeV confirmed the anomaly by extracting elliptic flow coefficient, v_2 , mass ordering of $v_2(p_T)$ for identified charged particles [11] and p_T -dependence of v_2 [9]. Similar unexpected features of particle production have also been observed in pPb collisions at $\sqrt{s_{NN}} = 5.02$ TeV [12–15] at the LHC. Subsequently, the RHIC data of dAu collisions uphold [16] the LHC observation of collective property in particle production from small systems. The observation of elliptic and triangular flow patterns of charged particles produced in pAu, dAu and $^3\text{HeAu}$ collisions at $\sqrt{s_{NN}} = 200$ GeV have been

reported [17] to be described best by hydrodynamic models, which include the formation of a short-lived QGP droplet. Theoretically, the appearance of “ridge” structure in high-multiplicity pp events at 7 TeV has been shown [18] to be expected in hydrodynamic approach, based on flux tube initial conditions. The observation of the collective behaviour of particle production in high-multiplicity pp events was further corroborated with the strong transverse radial flow extracted [19] from satisfactory description of identified charged particle yields [20] from high-multiplicity pp events by the hydrodynamics-motivated Boltzmann - Gibbs blast-wave (BGBW) model [21]. Several other theoretical and phenomenological studies [22–26] indicate the possibility of a hydro-like collective medium in high-multiplicity pp events. In spite of all these studies, suggesting collective behaviour of particle production in high-multiplicity events of small systems, the idea of connecting these anomalous features with the established hydro-like features of particle production from the QGP-like thermalized medium is not unanimously acceptable yet because of non-observance of the signal of suppression of high- p_T particles or any other compelling signal of formation of the medium. Further, while several models, in different approaches, qualitatively describe the data, it becomes difficult to conclude on physics origin of particle production. The source of the “collective” or the flow-like features in the small systems thus remains ambiguous and invite thorough studies involving quantitative comparison of the data in the light of several existing models of particle productions in relativistic pp collisions.

This article presents a comprehensive study on high-multiplicity pp events at $\sqrt{s} = 7$ and 13 TeV, comparing the data with EPOS3 [27] generated simulated events, with the aim to understand the anomalous features of particle production in pp collisions at the LHC. The EPOS3 simulation generates events with and without hydrodynamical evolution. The hydrodynamic EPOS3

*Electronic address: prem@vecc.gov.in

event generator follows similar particle production mechanism in *proton – proton*, *proton – nucleus* and *nucleus – nucleus* collisions and thus become a suitable testing ground for understanding the observed flow-like features in the high-multiplicity *pp* and *pPb* events at the LHC in comparison with the well studied collective phenomena in relativistic *nucleus – nucleus* collisions. In the following section, we describe the event generator, in brief. We analyse the EPOS3 generated events and present the results in Section III, in terms of the experimental observables which exhibit the flow-like effects in high-multiplicity *pp* events, namely i) the two-particle azimuthal correlations among charged particles, ii) the blast-wave description of identified charged particles iii) the mean transverse momentum ($\langle p_T \rangle$) as a function of mean charged multiplicity ($\langle N_{ch} \rangle$) and iv) the inverse slope parameter of transverse mass (m_T)-distribution. All these observables are related to the transverse momentum of produced particles, collectively presented as the inclusive charged particle transverse momentum spectra. Before carrying out differential analysis of the generated events in terms of these observables for a closer comparison with the data on an equal basis, the measured inclusive charged particle transverse momentum spectra for *pp* collisions at $\sqrt{s} = 7$ and 13 TeV are matched with those obtained from simulated events to ensure that the simulation code is, at least, minimally tuned. We summarise and conclude in Section IV.

II. EVENT GENERATOR

The detail of the EPOS3 model parameters are discussed in the ref. [27]. The model is known as Parton-based Gribov-Regge theory. In the Gribov-Regge multiple scattering framework, an individual scattering, referred to as Pomeron, gives rise to parton ladder that consists of a hard pQCD scattering along with initial-state and final-state parton emission. The parton ladder may be considered as a longitudinal color field or a flux tube, carrying transverse momentum of the hard scattering. The flux tubes expand and eventually get fragmented into string segments of quark-antiquark pairs. In case of many elementary parton-parton hard scattering in a collision, a large number of flux tubes are formed leading to a high local string-segment density, and subsequently high multiplicity of the collisional event. In the hydrodynamic EPOS3 model, the high local string-segment density, above a critical value, constitute the bulk matter or a medium. The string segments which do not have enough energy to escape from the bulk matter,

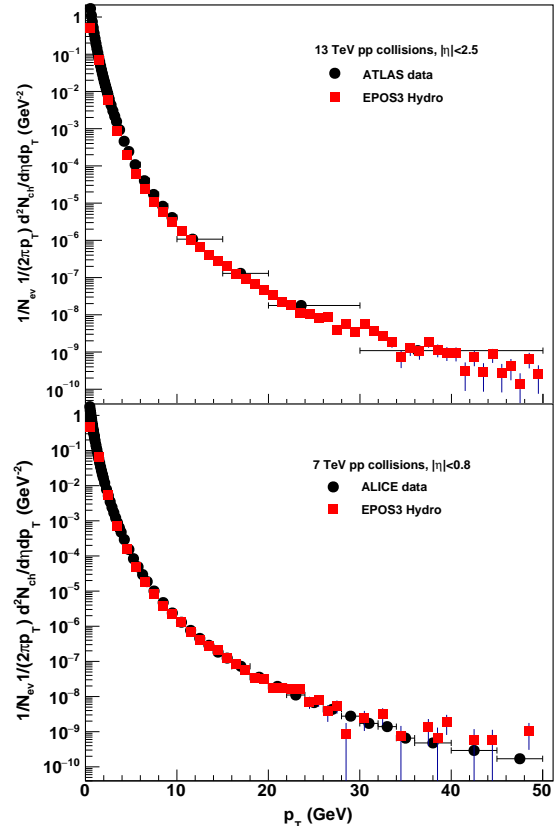


FIG. 1: Inclusive transverse momentum spectra of charged particles from generated minimum-bias events of *pp* collisions at $\sqrt{s} = 7$ and 13 TeV from EPOS3 event generator, with hydrodynamic calculations, are compared with data, as measured by ALICE [28] (lower panel) and ATLAS [29] (upper panel) experiments, respectively.

form the “core” that gets thermalized and undergoes (3 + 1D) viscous hydrodynamical evolution with a lattice QCD-complied cross-over equation of state and the ratio of the shear viscosity and entropy density, η/s is taken as 0.08. The hydrodynamical evolution is followed by particle production in Cooper-Frye mechanism. After that, the hadronic evolution takes place and the “soft” (low p_T) hadrons freeze-out. The string segments from outside the bulk matter form the “corona”. The string segments in the “corona” hadronize by Schwinger’s mechanism and escape as “high” p_T jet-hadrons. The string segments carrying enough energy to escape the bulk matter constitute the “semi-hard” or intermediate p_T particles. These segments, while escaping the bulk matter, pick-up quark or antiquark from within the bulk matter and the intermediate- p_T hadrons thus produced in this process, inherit the properties of the bulk matter. After hadronization, the hadron-hadron re-scattering

is modelled via UrQMD.

Using the EPOS 3.107 code, we have generated 40 million minimum-bias pp events for both the centre-of-mass energies, 7 and 13 TeV, for each of the options, with and without hydrodynamics. As presented in figure 1, our simulated event sample from the hydrodynamic EPOS3 successfully describe the inclusive charged particle spectra from pp collisions at $\sqrt{s} = 7$ [28] and 13 TeV [29]. We analyze same sample of events in terms of the discussed observables. Suitable subsamples of different multiplicity classes and different kinematic cuts are selected from the simulated minimum-bias event samples.

III. ANALYSIS AND RESULTS

A. Long-range ridge-like correlations

It will be pertinent to mention here, once again, that the “ridge-like” two-particle long-range angular correlations, a signal of collective behaviour of particle production in heavy-ion collisions, as observed in pp collision data at $\sqrt{s} = 7$ TeV, could be qualitatively generated [17] in “flux-tube + hydro” approach, similar to the approach adopted in EPOS code. In spite of the successes of the hydrodynamic approach in qualitative description, a quantitative comparison with the data is essential, particularly to access how the hydrodynamic description, implemented in EPOS, works better than the non-hydrodynamic models including the reasonably well understood particle production mechanism in the pQCD inspired multiple parton interaction (MPI) model, like the one implemented in PYTHIA Monte Carlo Code.

The two-particle angular correlation function is defined by the per-trigger associated yields of charged particles obtained from $\Delta\eta, \Delta\varphi$ distribution (where $\Delta\eta$ and $\Delta\varphi$ are the differences in the pseudo-rapidity (η) and azimuthal angle (φ) of the two particles) and is given by:

$$\frac{1}{N_{trig}} \frac{d^2 N_{assoc}}{d\Delta\eta d\Delta\varphi} = B(0,0) \times \frac{S(\Delta\eta, \Delta\varphi)}{B(\Delta\eta, \Delta\varphi)} \quad (1)$$

where N_{trig} is the number of trigger particles in the specified $p_T^{trigger}$ range.

The function $S(\Delta\eta, \Delta\varphi)$ is the differential measure of per-trigger distribution of associated hadrons in the same-event, i.e.,

$$S(\Delta\eta, \Delta\varphi) = \frac{1}{N_{trig}} \frac{d^2 N_{same}^{assoc}}{d\Delta\eta d\Delta\varphi} \quad (2)$$

The background distribution function $B(\Delta\eta, \Delta\varphi)$ is defined as:

$$B(\Delta\eta, \Delta\varphi) = \frac{d^2 N^{mixed}}{d\Delta\eta d\Delta\varphi} \quad (3)$$

where N^{mixed} is the number of mixed event pairs.

The factor $B(0,0)$ in Eqn. 1 is used to normalize the mixed-event correlation function such that it is unity at $(\Delta\eta, \Delta\varphi)=(0,0)$.

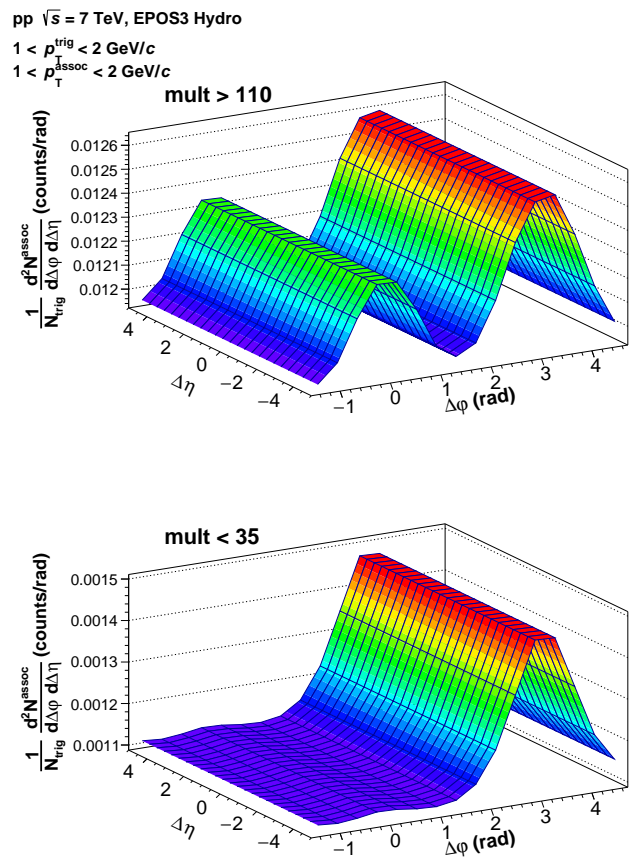


FIG. 2: Two particle $\Delta\eta - \Delta\varphi$ charge particle correlation function for $1 < p_T^{trigger}, p_T^{associated} < 2$ GeV/c with unidentified charged particle as trigger, for the hydrodynamic-EPOS3 generated pp collisions at $\sqrt{s} = 7$ TeV for events of multiplicity-class $N_{ch} > 110$ (upper panel) and $N_{ch} < 35$ (lower panel). The short-range correlations have been suppressed for clear presentation of the long-range correlations

The two-particle azimuthal correlations study helps extracting several sources of correlations in multiparticle production, depending on the studied

ranges of $|\Delta\eta|$ and also the p_T for the trigger and the associated particles. In the context of the present study, the correlated emission of particles from collective medium can be extracted by studying the long-range ($|\Delta\eta| \gg 0$) two-particle azimuthal angle correlations. In relativistic heavy-ion collisions, the long-range two-particle azimuthal angle correlations are attributed to the formation of collective medium. The correlated pair yields per trigger with small $|\Delta\varphi|$ over a wide range of $|\Delta\eta|$ (long-range), result a “ridge” structure in the constructed correlation functions. The analysis [10] of LHC pp data in terms of correlated yields as a function $|\Delta\varphi|$ reveals that the “ridge”-structure becomes prominent in pp collisions with increasing multiplicity of events. It is the near-side ($|\Delta\varphi| \sim 0$) long-range correlations, that are of particular interest for the present study of quantitative comparison of data and the hydrodynamic simulation of multi-particle production in high-multiplicity pp events.

We construct the long-range two-particle angular correlations of the charged particles in simulated events, matching the kinematic cuts and multiplicity classes as chosen for analysis of the data at references - [10] for $\sqrt{s} = 7$ and 13 TeV. As expected from a hydrodynamic code of particle production like the EPOS3-hydro, the long-range two-particle azimuthal correlations of charged particles reveal a prominent ridge-like structure for high-multiplicity events, while such structure is absent in low-multiplicity events. The figure 2 contains representative plots of two-particle correlation function for $1 < p_T^{trigger}, p_T^{associated} < 2$ GeV/c with unidentified charged particle as trigger, for the hydrodynamic-EPOS3 generated pp collisions at $\sqrt{s} = 7$ TeV for events of multiplicity-classes $N_{ch} > 110$ and $N_{ch} < 35$, after removing the short-range jet-like correlations. The per-trigger correlated yield, for representative high-multiplicity event classes, in different p_T -intervals, for both the non-hydrodynamic and hydrodynamic EPOS3 generated pp collisions at $\sqrt{s} = 7$ and 13 TeV are projected onto $\Delta\varphi$, after subtracting the “zero yield at minimum”, $Yield|_{ZYAM}$ [10], and are shown in the figure 3 and figure 4, respectively, to compare the data in the same kinematic ranges.

The appearance of the ridge-like structure in the long-range two-particle angular correlations of the charged particles in the high-multiplicity EPOS3-hydro generated pp events at $\sqrt{s} = 7$ and 13 TeV reflects the collective property, that is expected in a hydrodynamic model of particle production. The correlated yields of high-multiplicity event class as a function of $\Delta\varphi$ for different p_T -intervals in the simulated events reveals similar feature as observed in the two-particle azimuthal correlations of the charged particles in the

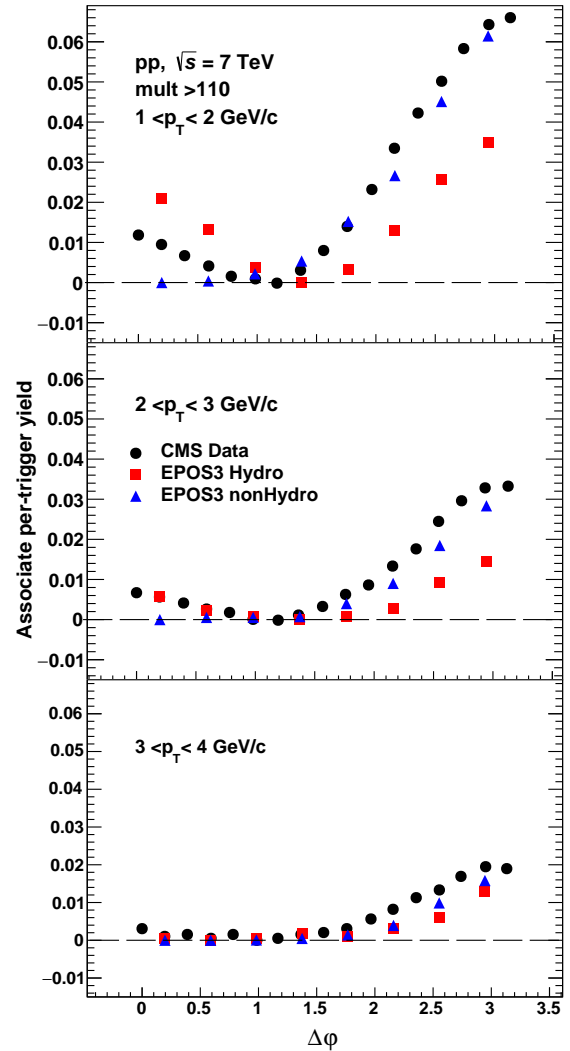


FIG. 3: One dimensional $\Delta\varphi$ projection for high-multiplicity events for the region of ridge-like correlations obtained from the long-range two-particle azimuthal correlations of charged particles, averaged over $2 < |\Delta\eta| < 4$, for $1 < p_T^{trigger}, p_T^{associated} < 2$ GeV/c, $2 < p_T^{trigger}, p_T^{associated} < 3$ GeV/c and $3 < p_T^{trigger}, p_T^{associated} < 4$ GeV/c from the data [10] and the hydrodynamic-EPOS3 generated events of pp collisions at $\sqrt{s} = 7$ TeV.

data: the ridge-like structure is most prominent in the 1 to 2 GeV/c p_T -range and in the highest-multiplicity events, while it gradually decreases with increasing p_T . Nevertheless, as it is clear in the figure 3 and figure 4, for the most prominent p_T -range of 1-2 GeV/c, the EPOS3 events overestimate the correlated yields as compared to the data.

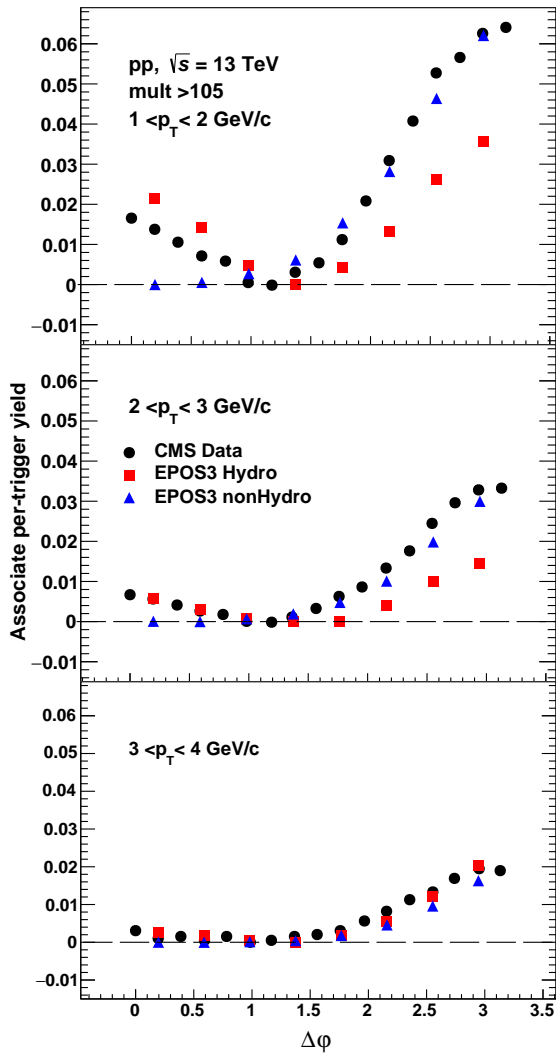


FIG. 4: Same as figure 3 for pp events at $\sqrt{s} = 13$ TeV.

B. Blast wave parametrization

In a hydrodynamic picture of relativistic collisions of heavy nuclei, the collective radial flow, generated due to the pressure gradient in the system, is reflected in the spectra of identified final state charged particles produced in relativistic collisions. The Boltzmann-Gibbs blast-wave (BGBW) [21] model, a hydrodynamics-motivated empirical formalism, estimates the radial flow by analyzing the identified particle spectra. The blast-wave model considers that the particles produced in the collision are locally thermalized and the system expands collectively with a common velocity field. Though model does not include hydrodynamic evolution, it considers that the system undergoes an instantaneous common freeze-out at a kinetic freeze-out temperature (T_{kin}) and a transverse radial flow velocity (β) at the freeze-out surface. The

BGBW, thoroughly used in analyzing the relativistic nucleus-nucleus collisions data, revealed [19] transverse radial flow for high-multiplicity pp collisions [20] data, also.

Assuming the hard-sphere particle source of uniform density, the transverse momentum spectra, in the BGBW model, is given by,

$$\frac{dN}{p_T dp_T} \propto \int_0^R r dr m_T \mathbf{I}_0 \left(\frac{p_T \sinh \rho}{T_{kin}} \right) \mathbf{K}_1 \left(\frac{m_T \cosh \rho}{T_{kin}} \right) \quad (4)$$

where $\rho = \tanh^{-1} \beta$, \mathbf{I}_0 and \mathbf{K}_1 are modified Bessel functions.

The flow velocity profile is given by,

$$\beta = \beta_s \left(\frac{r}{R} \right)^n \quad (5)$$

where β_s is the surface velocity and r/R is the relative radial position in the thermal source. The average transverse flow velocity, $\langle \beta \rangle$ is given by, $\langle \beta \rangle = \frac{2}{(2+n)} \beta_s$.

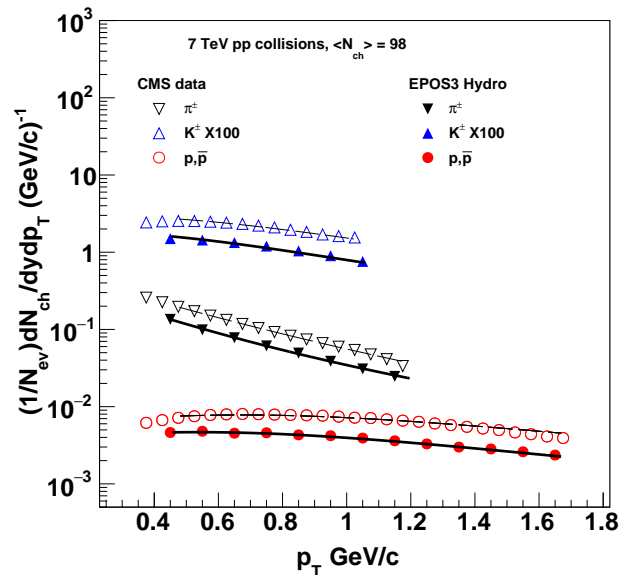


FIG. 5: The transverse momentum spectra for π^\pm , K^\pm , $p(\bar{p})$ as measured by the CMS experiment [20] at LHC for the event-class of average multiplicity = 98 in pp -collisions at $\sqrt{s} = 7$ TeV, along with BG-blast-wave fits (solid lines). The uncorrelated statistical and systematic uncertainties have been added in quadrature.

The hydrodynamic EPOS3 generated pp events are expected to exhibit the radial flow. Using the BGBW formalism, we intend to compare quantitatively the radial flow parameters for the EPOS3 generated events

and the data. We use the Chi-square (χ^2) test to ensure goodness of fit while obtaining the fit-parameters, the kinetic freeze-out temperature and the radial flow velocity, from the spectra data as well as from the generated spectra. For our analysis, we put lower p_T - cut at 0.475 GeV/c of spectra for all the species. At the higher side, the p_T -range is limited to $p_T < 2$ GeV/c or less, depending on the availability of the data.

We calculate R for different event classes with different $\langle N_{ch} \rangle$ in $|\eta| < 2.4$ in this study, from the relation, $R(\langle N_{ch} \rangle) = a \cdot \langle N_{ch} \rangle^{1/3}$ where $a = 0.597 \pm 0.009(stat.) \pm 0.057(syst.)$ fm at 0.9 TeV and $a = 0.612 \pm 0.007(stat.) \pm 0.068(syst.)$ fm, as parameterized [20] by the CMS experiment from the measurement of radius of source of emission as a function of average charged particle multiplicity for pp collisions at $\sqrt{s} = 7$ TeV. The BGBW fit parameters are available [19] for different multiplicity classes of pp collisions at $\sqrt{s} = 7$ TeV [20]. We fit the blast-wave function to the p_T - spectra for different sets of data for $\sqrt{s} = 13$ TeV [30], keeping the kinetic freeze-out temperature (T_{kin}), the radial flow velocity (β_s) and the exponent (n) of the flow velocity profile free to produce the best possible simultaneous or combined fits to the data, in terms of χ^2/ndf .

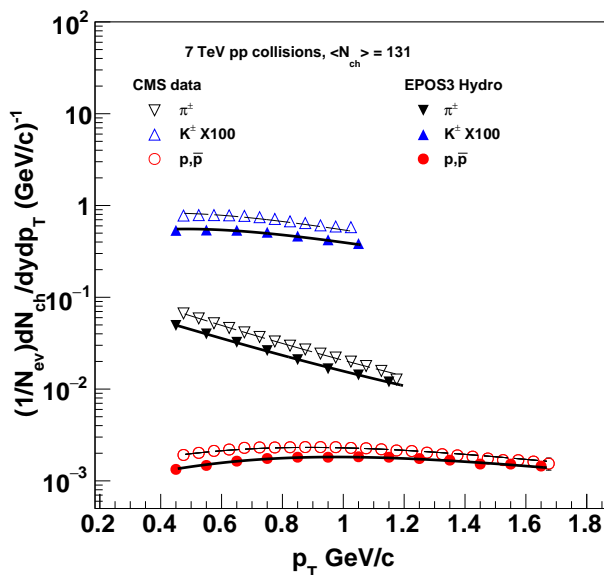


FIG. 6: The transverse momentum spectra for π^\pm , K^\pm , $p(\bar{p})$ as measured by the CMS experiment [20] at LHC for the event-class of average multiplicity = 131 in pp -collisions at $\sqrt{s} = 7$ TeV, along with BG-blast-wave fits (solid lines). The uncorrelated statistical and systematic uncertainties have been added in quadrature.

The figures 5 and 6 are representative plots where BGBW fits to the spectra data of identified particles from pp collisions at 7 TeV for the event-classes of average multiplicity = 98 and 131, respectively, are shown along with the fits to the simulated spectra, obtained from the respective class of simulated events.

$\sqrt{s}(TeV)$	$\langle N_{ch} \rangle$	$T_{kin}(MeV)$	$\langle \beta \rangle$	n	$\chi^2/n.d.f$
7	98	115.57 ± 0.11	0.766 ± 0.004	0.540 ± 0.006	1.02
7	109	113.09 ± 0.12	0.779 ± 0.004	0.503 ± 0.006	0.61
7	120	110.84 ± 0.15	0.790 ± 0.004	0.480 ± 0.006	0.34
7	131	104.29 ± 0.15	0.809 ± 0.005	0.436 ± 0.005	0.44
13	108	140.80 ± 0.022	0.723 ± 0.005	0.58 ± 0.01	1.65
13	119	129.31 ± 0.019	0.778 ± 0.002	0.56 ± 0.011	0.86
13	130	128.29 ± 0.019	0.763 ± 0.004	0.50 ± 0.009	1.18
13	141	119.77 ± 0.016	0.764 ± 0.004	0.48 ± 0.01	1.40
13	151	112.84 ± 0.016	0.783 ± 0.004	0.44 ± 0.011	1.44
13	162	102.67 ± 0.017	0.826 ± 0.003	0.36 ± 0.007	0.93

TABLE I: T_{kin} , $\langle \beta \rangle$ and n , the parameters of the the BGBW, obtained from the simultaneous fit to the published [20, 29] spectra of π^\pm , K^\pm and $p(\bar{p})$ and respective $\chi^2/n.d.f$ for pp collisions at $\sqrt{s} = 7$ and 13 TeV for different event classes depending on average multiplicity, $\langle N_{ch} \rangle$, in the range $|\eta| < 2.4$.

We tabulate the fit parameters, the kinetic freeze-out temperature (T_{kin}), the average radial flow velocity ($\langle \beta \rangle$) at the freeze-out surface, and the exponent (n) as obtained by simultaneous fit of identified particle spectra by BGBW for different classes of high-multiplicity pp events and for $\sqrt{s} = 7$ and 13 TeV, along with respective $\chi^2/n.d.f$ in table I. The table includes parameters for those event classes which fit reasonably with the BW function. The table II presents similar results for the EPOS3-hydro model generated events.

The figures 5 and 6 along with the tables I and II show that the data and the EPOS3-hydro generated events are far from quantitative agreement, in terms of the BW-parameters, except for very-high multiplicity classes of average multiplicity = 151 and 162 in pp -collisions at $\sqrt{s} = 13$ TeV.

C. The $\langle p_T \rangle$ as a function of $\langle N_{ch} \rangle$

The ALICE experiment at the LHC measured [31] on $\langle p_T \rangle$ of charged particles, in the pseudorapidity range $|\eta| < 1.0$ and with the transverse momentum, p_T up to 10 GeV/c, as a function of $\langle N_{ch} \rangle$ and showed that data of pp collisions at $\sqrt{s} = 7$ TeV could be well described by the pQCD-inspired multiple parton interaction (MPI) model with color reconnection, as implemented in PYTHIA monte carlo code. We calculate the observables, in the the same kinematic ranges used by the ALICE, for the events generated with both the hydro and non-hydro EPOS3 simulations.

$\sqrt{s}(\text{TeV})$	$\langle N_{ch} \rangle$	$T_{kin}(\text{MeV})$	$\langle \beta \rangle$	n	$\chi^2/n.d.f$
7	98	106.10 ± 0.015	0.768 ± 0.0003	0.59 ± 0.001	30.83
7	109	105.91 ± 0.008	0.808 ± 0.001	0.46 ± 0.005	1.51
7	120	103.30 ± 0.01	0.813 ± 0.002	0.45 ± 0.003	1.59
7	131	103.02 ± 0.02	0.829 ± 0.002	0.39 ± 0.004	0.52
13	108	142.00 ± 0.002	0.749 ± 0.001	0.63 ± 0.01	7.54
13	119	142.00 ± 0.0019	0.774 ± 0.005	0.50 ± 0.002	0.86
13	130	141.96 ± 0.006	0.774 ± 0.008	0.45 ± 0.009	1.16
13	141	127.98 ± 0.016	0.797 ± 0.001	0.44 ± 0.004	1.31
13	151	112.90 ± 0.01	0.814 ± 0.006	0.43 ± 0.004	0.96
13	162	100.52 ± 0.015	0.815 ± 0.007	0.42 ± 0.007	1.43

TABLE II: T_{kin} , $\langle \beta \rangle$ and n , the parameters of the the BGBW, obtained from the simultaneous fit to the spectra obtained from simulated EPOS events for π^\pm , K^\pm and $p(\bar{p})$ and respective $\chi^2/n.d.f$ for pp collisions at $\sqrt{s} = 7$ and 13 TeV for different event classes depending on average multiplicity, $\langle N_{ch} \rangle$, in the range $|\eta| < 2.4$.

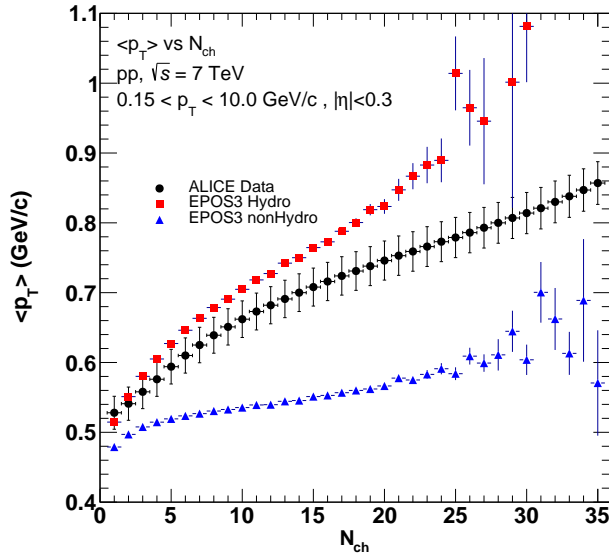


FIG. 7: Average transverse momentum, $\langle p_T \rangle$, as a function of charged particle multiplicity, N_{ch} , as measured [31] by ALICE is compared with the simulated events from EPOS3 event generator, with and without Hydro calculations.

The results are depicted in the plots, along with the data in Fig. 7.

As is clear from Fig. 7, the EPOS3 code, with or without hydrodynamics, cannot describe the ALICE measurement of $\langle p_T \rangle$ as a function of $\langle N_{ch} \rangle$. The ATLAS experiment has studied [28] the same for pp collisions at $\sqrt{s} = 13$ TeV, though in different kinematic ranges, $|\eta| < 2.4$ and $p_T > 0.5$ GeV/c. We repeat the $\langle p_T \rangle$ as a function of $\langle N_{ch} \rangle$ analysis

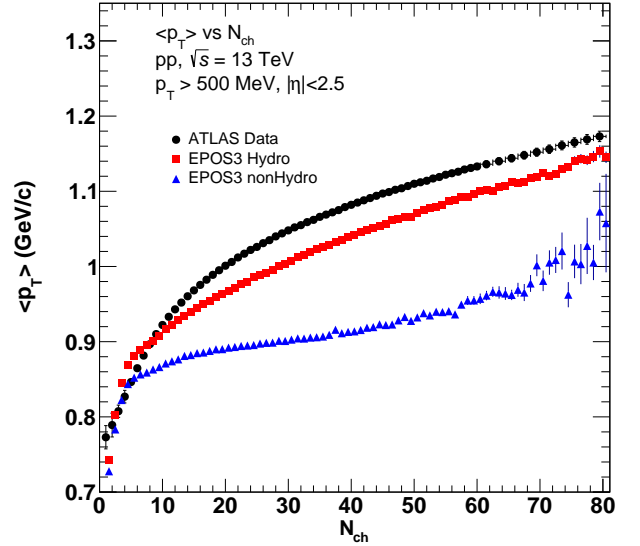


FIG. 8: Average transverse momentum, $\langle p_T \rangle$, as a function of charged particle multiplicity, N_{ch} , as measured [28] by ATLAS is compared with the simulated events from EPOS3 event generator, with and without Hydro calculations.

in accordance with the kinematic cuts used for the ATLAS data. The comparison of the simulation and the data is presented in Fig. 8. In this case also the data and the simulated events vary widely. It may be noted that both the ALICE and the ATLAS data includes particles of p_T , much higher than the p_T -range of the “soft” particles likely to be produced from the “core” or the bulk collective medium that is considered in the EPOS hydrodynamic code. In view of this, to compare the data with “soft” particles only, we choose the CMS data on identified p_T -spectra from events of different multiplicity classes.

The CMS experiment has measured p_T -spectra of π^\pm , K^\pm , $p(\bar{p})$ over the rapidity, $(y = (1/2)\ln\frac{E+p_L}{E-p_L})$ range $|y| < 1$ for the pp collisions at $\sqrt{s} = 7$ and 13 TeV $|\eta| < 2.4$. The measured p_T - ranges for the measured identified particles in the pp collisions at both the energies, 7 TeV [20] and 13 TeV [30] are 0.1 to 1.2 GeV/c for π^\pm , 0.2 to 1.050 GeV/c for K^\pm and 0.35 - 1.7 GeV/c for p and \bar{p} . The measured p_T -ranges fall within the p_T - range of EPOS3 for particles originating from hydrodynamic bulk medium.

We compute $\langle p_T \rangle$ from the CMS data on identified charged particle spectra for different event classes from pp collisions at $\sqrt{s} = 7$ [20] and 13 [30] TeV. It

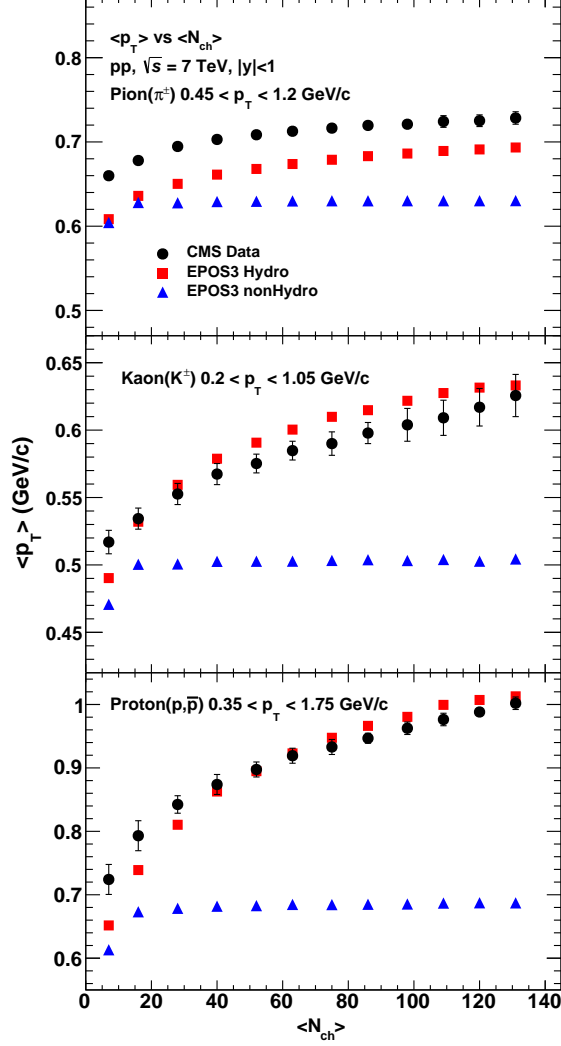


FIG. 9: Average transverse momentum, $\langle p_T \rangle$, as a function of mean charged particle multiplicity, $\langle N_{ch} \rangle$, for the identified particles in pp collisions at $\sqrt{s} = 7$ TeV. The CMS data [20], have been compared with simulated events using EPOS3 event generator with and without hydrodynamics.

is clear from figure. 9 that for pp collisions data at 7 TeV, the $\langle p_T \rangle$ of majority of produced “soft” particles, the pions, for the simulated events do not match the measured ones in the given kinematic range. For the pp collisions at 13 TeV, the mismatch between the data and the simulated events, as shown in figure 10, is quite wide for all the identified particles.

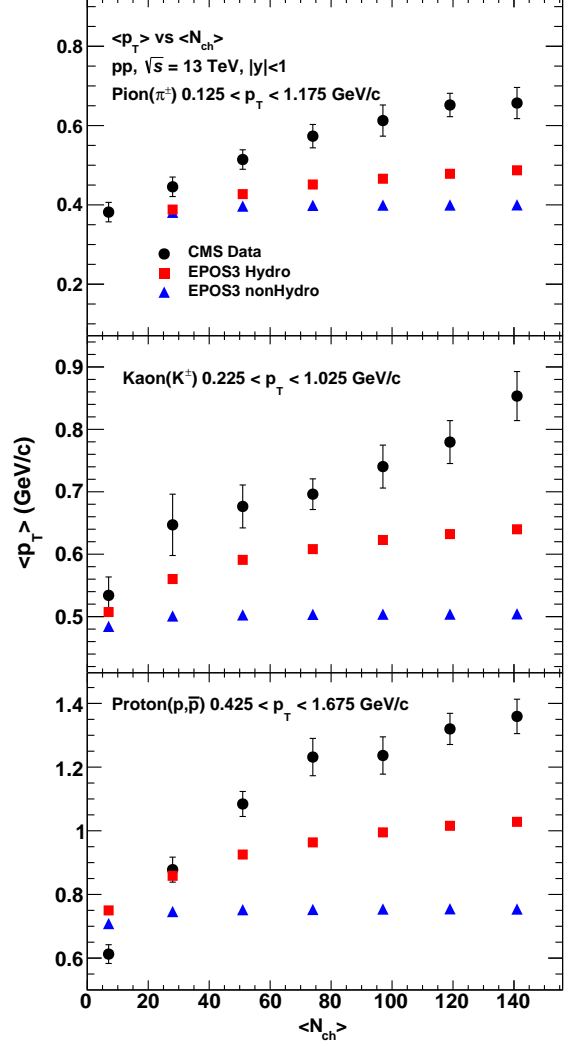


FIG. 10: Average transverse momentum, $\langle p_T \rangle$, as a function of mean charged particle multiplicity, $\langle N_{ch} \rangle$, for the identified charged particles in pp collisions at $\sqrt{s} = 13$ TeV. The CMS data [30], have been compared with simulated events using EPOS3 event generator with and without hydrodynamics.

D. Multiplicity dependent inverse slope parameter of m_T -distributions

The slope of transverse mass m_T -spectra of identified particle contains information of temperature of a medium, if formed, from where the particles are produced, and the effect of transverse expansion of the medium. We obtain the m_T spectra of identified charged particle of mass m for different high-multiplicity classes of pp events at $\sqrt{s} = 7$ and 13 TeV from the p_T -spectra measured [20, 30] by the CMS experiments from the relation, $m_T = (m^2 + p_T^2)^{1/2}$.

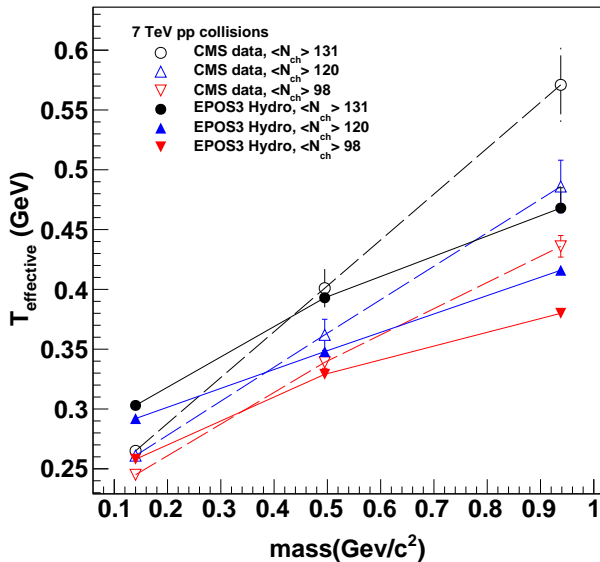


FIG. 11: The mass ordering of the inverse slope parameter $T_{effective}$ of identified particles ($m_{\pi^\pm} = 0.14$, $m_{K^\pm} = 0.495$, $m_{p(\bar{p})} = 0.938 \text{ GeV}/c^2$) as measured by the CMS experiment [20] at $\sqrt{s} = 7 \text{ TeV}$, for a few event classes of high-multiplicity, is compared with those obtained from EPOS3-hydro simulated events. The $\langle N_{ch} \rangle$ is the mean multiplicity of the charged particles of respective event-class.

The m_T -spectra are fitted, in the range corresponding to low- p_T , with the exponential function:

$$\frac{dN}{m_T dm_T} = C \cdot \exp\left(-\frac{m_T}{T_{effective}}\right) \quad (6)$$

where $T_{effective}$, the inverse slope parameter, contains the effect due to the transverse expansion of the system. The increase in the inverse slope parameter, $T_{effective}$ for the most commonly measured identified particles (π^\pm , K^\pm , p and \bar{p}), as has been observed in heavy-ion collisions [32, 33] is attributed to the collective transverse flow of the medium formed in the collision. The increase in inverse slope parameters has also been observed in high-multiplicity event classes of pPb collisions at $\sqrt{s_{NN}} = 5.02 \text{ TeV}$ [34] and pp collisions at $\sqrt{s} = 7$ [35].

We fit the m_T - spectra of identified particles in the overlapped range ($0.475 < p_T < 1.025$) of p_T - spectra at $\sqrt{s} = 7$ and 13 TeV , obtained from the data [20, 30] as well as from the EPOS3-hydro simulation

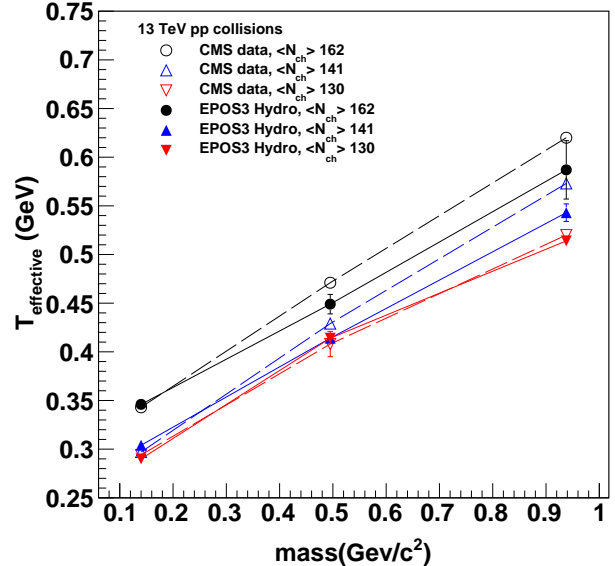


FIG. 12: Same as figure 11 for measured CMS data [30] and EPOS3 simulated events of pp collisions at $\sqrt{s} = 13 \text{ TeV}$

for the high-multiplicity event classes. The inverse slope parameters, obtained from the best fit of the spectra, in terms of χ^2/ndf , using the MINUTE program in the ROOT analysis framework [29] are presented in figures 11 and 12 for some representative high-multiplicity event-classes

From the figures 11 and 12, it is clear that while the EPOS3-hydro high-multiplicity pp events exhibit mass ordering of inverse slope parameter of the m_T - distributions, they largely deviate from the ones obtained from the measured spectra.

IV. SUMMARY AND CONCLUSION

In the context of several experimental signatures of collective nature of particle productions in relativistic collisions of small systems at RHIC and LHC, we analyse simulated pp events at $\sqrt{s} = 7$ and 13 TeV from EPOS3-hydro code, a hydrodynamic model of particle production in different systems of relativistic collisions, for quantitative comparisons with the particle production data in high-multiplicity pp events for better understanding of the experimental signals.

We have studied the multiplicity dependence of the long-range two-particle angular correlations of charged particles, produced in EPOS3-generated pp events. The EPOS3-hydro generated high-multiplicity

events reveal the “ridge-like” structure, that is most prominent in the 1 to 2 GeV/c p_T -range, while it gradually decreases with increasing p_T -interval. The diminishing trend of correlated yield with the increasing p_T -interval is similar to what is observed in data. However, the EPOS3 events overestimate the correlated yields. The kinetic freeze-out temperature (T_{kin}) and a transverse radial flow velocity (β) at the freeze-out surface as obtained from the blast-wave fits to the identified particle spectra for high-multiplicity event classes of EPOS3-simulated events, do not match those parameters for the data. The mean transverse momentum as a function of multiplicity for all charged particle and as a function of mean multiplicity for identified charged particles from EPOS3 generated events, in different kinematic ranges, vary widely from those measured for 13 TeV pp data at LHC. The inverse slope parameters obtained by exponential fits to the transverse mass spectra of EPOS3 generated events, though exhibiting mass-ordering as expected in hydrodynamic model of particle production, the values of the parameter do not agree with those obtained from the data.

This data-driven study reveals that though the EPOS3 hydrodynamic model may reasonably describe the nature of some of the average bulk features, reflecting collective properties of particle production in the high-multiplicity pp events at the LHC, it cannot match the data quantitatively. With the quantitative mismatch in terms of the studied observables, related to the transverse momentum of the particles, one would expect a quantitative mismatch in terms of the fundamental observable, the inclusive spectra of invariant yields of produced particles, also. In this respect, the EPOS3 code appears inconsistent. The quantitative mismatch, however, cannot undermine the qualitative agreement of the EPOS3 simulation with the data. As has already been shown [35] in a study on identified particle spectra data [20] of pp collisions at 7 TeV, both the EPOS versions, EPOS3 and EPOS-LHC, match the trend of the data better than the conventional non-hydro event generators, including PYTHIA [36]. The EPOS simulations, in contrast to PYTHIA, include flow of produced particles. The EPOS-LHC contains parameterized collective flow at the freeze-out and EPOS3, the advance version, contains a full (3D + 1) viscous hydrodynamic simulation. The better matching of the particle spectra data by EPOS simulations as compared to the conventional pp simulation codes establishes the collective behaviour of pp data at the LHC. Nevertheless, in the scenario when several other hydrodynamic as well as non-hydrodynamic models qualitatively reproduce the so-called collective features of particle productions in high-multiplicity small collision systems, quantitative descriptions of as many observables as possible in a

consistent framework / model is desirable, to identify the origin of these features. This study may be useful in tuning the EPOS3 input parameters further, to match the high-multiplicity pp data.

In the context of this study, it is worth noting that some other hydro-based calculations have reported good agreement with a few observables of high-multiplicity events of small collision systems. Considering fluctuating proton IP-Glasma initial state model coupled to viscous hydrodynamic simulations, followed by the hadronic cascade model UrQMD, the harmonic flow coefficients of the pPb data at $\sqrt{s_{NN}} = 5.02$ TeV could be well reproduced [37]. In another study [38], in a viscous hydrodynamic model, the collective features of high-multiplicity events data of pPb collisions at LHC and (p,d,³H)Au collisions at RHIC have been quantitatively matched. A common hydrodynamic origin to the experimentally observed flow of produced particles has been suggested [39] for all the large or the small central collision systems, including pp, pPb and PbPb at the LHC by considering a generalised initial condition calculations in the Glauber Model at the sub-nucleonic level, followed by a hybrid model that combines pre-equilibrium dynamics with viscous fluid dynamic evolution and late-stage hadronic re-scatterings.

On the other hand, some of the non-hydrodynamic models of particle productions also qualitatively match certain bulk collective features of high-multiplicity pp events. The Color Glass Condensate (CGC) effective theory also explains several of the experimental observations, including azimuthal correlations, of high-multiplicity small collision systems. In the IP-Glasma model, based on colour glass condensate, followed by the Lund string fragmentation algorithm of PYTHIA, with further tuning of the p_T -smearing fragmentation parameter in the default PYTHIA, the particle mass dependence of $\langle p_T \rangle$ and the p_T dependence of v_2 for pp collisions could be qualitatively reproduced [40]. The literature also provide some other sources of long-range rapidity correlations, beyond hydrodynamic or CGC models, in terms of initial state physics processes. Several sources of such long-range azimuthal correlations have been discussed in the review articles at references [41] and [42]. The ALICE measurement of $\langle p_T \rangle$ of the charged particles as a function of N_{ch} , including particles of p_T up to 10 GeV/c from pp collisions at 7 TeV, could be well reproduced [31] by invoking Colour Reconnection mechanism in PYTHIA (while EPOS3 remain far away from the data). The MPI model, however, cannot explain [35] the dependence of $\langle p_T \rangle$ on $\langle N_{ch} \rangle$ or does not provide alternate explanations to other important features of particle production in high-multiplicity events pp collisions at 7 TeV when the p_T -range is restricted to the range of interest for

studying the hydrodynamic collectivity.

The present study is consistent with ALICE study [43] that observes the EPOS3 event generator is tuned to the LHC Run 1 data, to describe the inclusive transverse momentum spectrum for 13 TeV pp collisions reasonably well but not in detail. Similarly, no particle production model, hydrodynamic or non-hydrodynamic, could quantitatively match all the collective features of the high-multiplicity pp data, while the high-multiplicity proton-nucleus data have been better matched by several models [37–40, 44], including EPOS3. We, thus, conclude that the observed anomaly in particle production in high-multiplicity pp events at the LHC still remains unresolved, inviting

further tuning of the existing models for quantitative description of the data.

V. ACKNOWLEDGEMENT

The authors are thankful to Klaus Werner for providing them with the EPOS3 code. The authors also thank the members of the computing teams of the KANNAD of the C&I Group of VECC for providing uninterrupted facility for event generation.

-
- [1] S. Z. Belenky and L. D. Landau, *Nuovo. Cim. Suppl.* **3**, 15 (1956).
- [2] I. Arsene et al., BRAHMS Collaboration, *Nucl. Phys.* **A757**, 1 (2005).
- [3] B. B. Back et al., PHOBOS Collaboration, *Nucl. Phys.* **A757**, 28 (2005).
- [4] J. Adams et al., STAR Collaboration, *Nucl. Phys.* **A757**, 102 (2005).
- [5] K. Adcox et al., PHENIX Collaboration, *Nucl. Phys.* **A757**, 184 (2005).
- [6] J. C. Collins and M. J. Perry, *Phys. Rev. Lett.* **34**, 1353 (1975).
- [7] E. Shuryak, *Phys. Rep.* **61**, 71 (1980).
- [8] V. Khachatryan et al., CMS Collaboration, *J. High Energy Phys.* **09**, 091 (2010).
- [9] G. Aad et al., ATLAS Collaboration, *Phys. Rev. Lett.* **116**, 172301 (2016).
- [10] V. Khachatryan et al., CMS Collaboration, *Phys. Rev. Lett.* **116**, 172302 (2016).
- [11] V. Khachatryan et al., CMS Collaboration, *Phys. Lett.* **B765**, 193 (2017).
- [12] B. Abelev et al., ALICE Collaboration, *Phys. Lett.* **B719**, 29 (2013).
- [13] S. Chatrchyan et al., CMS Collaboration, *Phys. Lett.* **B718**, 795 (2013).
- [14] G. Aad et al., ATLAS Collaboration, *Phys. Rev. Lett.* **110**, 182302 (2013).
- [15] B. Abelev et al., ALICE Collaboration, *Phys. Lett.* **B728**, 25(2014).
- [16] A. Adare et al., PHENIX Collaboration, *Phys. Rev. Lett.* **114**, 192301(2015).
- [17] A. Adare et al., PHENIX Collaboration, *Nature Physics.* (2018).
- [18] K. Werner, Iu. Karpenko, and T. Pierog, *Phys. Rev. Lett.* **106**, 122004 (2011).
- [19] P. Ghosh, S. Muhuri, J. Nayak, and R. Varma, *J. Phys.* **G41**, 035106 (2014).
- [20] V. Khachatryan et al., CMS Collaboration, *Euro. Phys. J.* **C72** 2164 (2012).
- [21] E. Schnedermann, J. Sollfrank and U. W. Heinz, *Phys. Rev.* **C48** 2462 (1993).
- [22] P. Bozek, *Eur. Phys. J.* **C71**, 1530 (2011).
- [23] R. Campanini and G. Ferri, *Phys. Lett.* **B703**, 237 (2011).
- [24] A. Kisiel, *Phys. Rev.* **C84**, 044913 (2011).
- [25] E. Shuryak and I. Zahed, *Phys. Rev.* **C88**, 044915 (2013).
- [26] I. Bautista, A. F. Tellez, and P. Ghosh, *Phys. Rev.* **D92**, 071504(R) (2015).
- [27] K. Werner, B. Guiot, Iu. Karpenko and T. Pierog, *Phys. Rev.* **C89**, 064903 (2014).
- [28] B. Abelev et al., ALICE Collaboration, *Eur. Phys. J.* **C73**, 2662 (2013).
- [29] G. Aad et al., ATLAS Collaboration, *Phys. Lett.* **B758**, 67 (2016).
- [30] A.M. Sirunyan et al., CMS Collaboration, *Phys. Rev.* **D96**, 112003 (2017)
- [31] B. Abelev et al. (ALICE Collaboration), *Phys. Lett.* **B727**, 371 (2013).
- [32] Bearden, I. G. et al., NA44 Collaboration. *Phys. Rev. Lett.* **78**, 2080 (1997).
- [33] Xu, N. *Prog. Part. Nucl. Phys.* **53**, 165 (2004).
- [34] S. Chatrchyan, et al., CMS Collaboration, *Eur. Phys. J.* **C74**, 2847 (2014).
- [35] S. Kar, S. Choudhury, S. Muhuri and P. Ghosh, *Phys. Rev.* **D95**, 014016 (2017).
- [36] T. Sjostrand, S. Mrenna, and P. Skands, *J. High Energy Phys.* **05**, 026 (2006).
- [37] H. Mntysaari, B. Schenke, C. Shen and P. Tribedy, *Phys. Lett.* **B772** 681 (2017).
- [38] C. Shen, J-F. Paquet, G. S. Denicol, S. Jeon, and C. Gale, *Phys. Rev.* **C95**, 014906 (2017).
- [39] R. D. Weller and P. Romatschke, arXiv:1701.07145v1 [nucl-th]
- [40] B. Schenke, S. Schlichting, P. Tribedy and Raju. Venugopalan, *Phys. Rev. Lett.* **117**, 162301 (2016).
- [41] K. Dusling, W. Li and B. Schenke, *Int. J. Mod. Phys.* **E25**, 1630002 (2016).
- [42] S. Schlichting and P. Tribedy, *Adv. High. Energy Phys.* 8460349 (2016).
- [43] J. Adam et al. (ALICE Collaboration), *Phys. Lett.* **B753**, 319 (2016).
- [44] S. Kar, S. Choudhury, S. Sadhu, and P. Ghosh, *J. Phys.* **G45**, 125103 (2018).